

Tbx6-dependent Sox2 regulation determines neural or mesodermal fate in axial stem cells

Tatsuya Takemoto¹, Masanori Uchikawa¹, Megumi Yoshida¹, Donald M. Bell², Robin Lovell-Badge², Virginia E. Papaioannou³ & Hisato Kondoh¹

The classical view of neural plate development held that it arises from the ectoderm, after its separation from the mesodermal and endodermal lineages. However, recent cell-lineage-tracing experiments indicate that the caudal neural plate and paraxial mesoderm are generated from common bipotential axial stem cells originating from the caudal lateral epiblast^{1,2}. *Tbx6* null mutant mouse embryos which produce ectopic neural tubes at the expense of paraxial mesoderm³ must provide a clue to the regulatory mechanism underlying this neural versus mesodermal fate choice. Here we demonstrate that *Tbx6*-dependent regulation of *Sox2* determines the fate of axial stem cells. In wild-type embryos, enhancer N1 of the neural primordial gene *Sox2* is activated in the caudal lateral epiblast, and the cells staying in the superficial layer sustain N1 activity and activate *Sox2* expression in the neural plate^{4–6}. In contrast, the cells destined to become mesoderm activate *Tbx6* and turn off enhancer N1 before migrating into the paraxial mesoderm compartment. In *Tbx6* mutant embryos, however, enhancer N1 activity persists in the paraxial mesoderm compartment, eliciting ectopic *Sox2* activation and transforming the paraxial mesoderm into neural tubes. An enhancer-N1-specific deletion mutation introduced into *Tbx6* mutant embryos prevented this *Sox2* activation in the mesodermal compartment and subsequent development of ectopic neural tubes, indicating that *Tbx6* regulates *Sox2* via enhancer N1. *Tbx6*-dependent repression of *Wnt3a* in the paraxial mesodermal compartment is implicated in this regulatory process. Paraxial mesoderm-specific misexpression of a *Sox2* transgene in wild-type embryos resulted in ectopic neural tube development. Thus, *Tbx6* represses *Sox2* by inactivating enhancer N1 to inhibit neural development, and this is an essential step for the specification of paraxial mesoderm from the axial stem cells.

Evidence derived from cell marking and lineage tracing in mouse and chicken embryos indicates that the caudal lateral epiblast (CLE), the region of epiblast flanking the rostral primitive streak, serves as the common precursor pool for the paraxial mesoderm and caudal neural plate which later contributes to the caudal hindbrain and spinal cord^{1,2,7}. The bipotential precursors serve as the pool of ‘axial stem cells’ that contributes to the coordinated elongation of the neural tube—which develops from the cell population remaining in the superficial layer—and paraxial mesoderm derived from cells that ingress through the primitive streak^{8–10}. The most compelling evidence for this was provided by the single cell lineage analysis reported by a previous study⁸, which used intragenic recombination in a transgene to mark a clone, and demonstrated that a substantial fraction of individual axial stem cells do produce progenies of both cell fates. However, the regulatory mechanism underlying this neural versus mesodermal fate choice remained to be elucidated.

Expression of the transcription factor gene *Sox2* is regarded as the hallmark of the neural primordial cell state, and its activation is strongly correlated with the establishment of the embryonic neural plate (Fig. 1b

and Supplementary Fig. 1). Our earlier studies have indicated that among a number of enhancers regulating *Sox2*, enhancer N1 is responsible for *Sox2* activation in the caudally extending neural plate^{5,6} (Fig. 1a–c and Supplementary Fig. 1). The following three features of enhancer N1 indicate its involvement in the regulation of CLE-derived cells⁴. First, enhancer N1 is activated precisely in the region of the CLE and sustained in the zone at the caudal end of neural plate (ZCNP) (Fig. 1b, c). Its activation, however, does not immediately lead to *Sox2* expression in the CLE, owing to BMP signal-dependent repression of *Sox2* in the CLE. Only when the CLE cells become a part of ZCNP located immediately rostral are the cells relieved from the BMP signal and initiate *Sox2* expression. In fact, the inhibition of BMP signals results in precocious *Sox2* activation in the entire CLE⁴ (Supplementary Fig. 2). Second, enhancer N1 activity is normally shut off in the mesodermal precursors that have ingressed through the primitive streak, indicative of the release of this cell population from a neural fate⁴. Third, enhancer N1 is activated by the synergistic action of Wnt and Fgf signals⁴ (Fig. 1d, e), whereas the Fgf signal is required for the

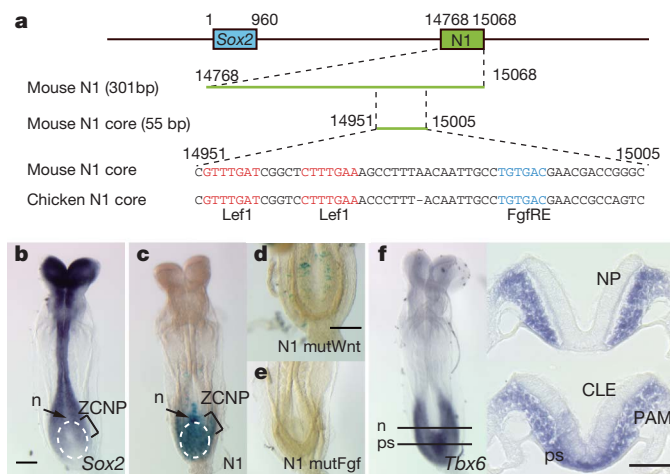


Figure 1 | Enhancer N1 of the mouse *Sox2* gene and its activity in comparison with *Sox2* and *Tbx6* expression. **a**, The position of enhancer N1 relative to the *Sox2* ORF and the N1 core sequence bearing the conserved Lef1-binding elements and Fgf-responsive element (FgfRE). **b**, Expression of *Sox2* in E8.5 normal embryo in dorsal view. **c**, Enhancer N1 activity at the same stage, indicated by the expression of enhancer N1-LacZ transgene in primary transgenic embryos. n, the position of node; ZCNP, zone at the caudal end of neural plate; dashed oval, the area of enhancer N1 activity. **d**, **e**, The loss of enhancer activity by the mutations in both Lef1 elements (**d**, mutWnt) or in FgfRE (**e**, mutFgf)⁴ in the transgenic embryos. **f**, *Tbx6* expression in E8.5 mouse embryo detected by *in situ* hybridization. The right panels show the cross-sections at the node (n; top panel) and primitive streak (ps; bottom panel) levels. CLE, caudal lateral epiblast; NP, neural plate; PAM, paraxial mesoderm. Scale bars: 200 μm (**b**–**e**); 50 μm (**f**, right panels).

¹Graduate School of Frontier Biosciences, Osaka University, 1-3 Yamadaoka, Suita, Osaka 565-0871, Japan. ²Division of Stem Cell Biology and Developmental Genetics, MRC National Institute for Medical Research, The Ridgeway, Mill Hill, London NW7 1AA, UK. ³Department of Genetics and Development, College of Physicians and Surgeons of Columbia University, 701 West 168th Street, New York, New York 10032, USA.

maintenance of the axial stem cells in the CLE^{1,11,12}. On the basis of these observations, we hypothesized that regulation of *Sox2* through enhancer N1 is an important mechanism to regulate cell fate in the CLE.

Given the CLE origin of paraxial mesoderm, the phenotype of *Tbx6* null mutant embryos is remarkable, where bilateral ectopic neural tubes develop at the expense of the paraxial mesoderm caudal to somite 6 level³. *Tbx6*, encoding a T-box transcription factor, is expressed in the primitive streak and presomitic paraxial mesoderm during gastrulation¹³ (Fig. 1f), and is presumed to have two major regulatory functions: (1) antineural fate regulation in the presomitic mesoderm, as indicated by the mutant phenotype; and (2) regulation of later somite segmentation involving *Mesp2* and *Dll1* genes^{14–17}.

We investigated the process of ectopic neural tube development from the presumptive paraxial mesoderm in homozygous *Tbx6* mutant embryos. In *Tbx6* mutant embryos at embryonic day (E)8.5, mesoderm development is already defective, as indicated by the absence of the normal pattern of *Uncx4.1* (also called *Uncx*) expression in the caudal part of segmented somites (Supplementary Fig. 3a). The expression of *Sox2* in normal embryos at E8.5 (5–6 somites) was confined to the neural plate and neural tube (Fig. 2a), whereas in *Tbx6* mutant embryos, the cells in the paraxial mesodermal compartment underlying the neural plate fully expressed *Sox2*, at levels comparable to those in the neural plate (Fig. 2b). The ectopic *Sox2* expression was followed by the ectopic development of neural tubes in the same compartment at E9.5 (Fig. 2c, d), where genes such as *Pax6* and *Pax3* were expressed, indicating the development of the dorso-ventral patterning of the ectopic neural tubes³ (see also Fig. 3).

In contrast to *Sox2*, other group B1 *Sox* genes—that is, *Sox1* and *Sox3*, which are normally expressed in the neural tube—were not activated in the paraxial mesodermal compartment (Fig. 2e–h). This observation strongly suggests that the activation of *Sox2* in the paraxial mesodermal compartment is causative of ectopic neural tube development in *Tbx6* mutant embryos.

By analogy to the process of caudal neural plate development, we speculated involvement of enhancer N1 activation, leading to *Sox2* expression, in ectopic neural tube development in *Tbx6* mutant embryos. To test this model, we compared enhancer N1 activity in *Tbx6* mutant and wild-type embryos (Fig. 2i, j and Supplementary Fig. 3b) using enhancer-N1-driven transgenes for *Egfp* (for *in situ* hybridization detection of transcripts) or *lacZ* (for histochemical enzyme staining). In wild-type embryos, enhancer-N1-dependent *Egfp* expression was clearly detected in the CLE and primitive streak, but not in the paraxial mesodermal compartment (Fig. 2i). Analysis of serial sections indicated that enhancer N1 loses its activity after the cells ingress through the primitive streak and when the cells migrate laterally into the mesodermal compartment (Fig. 2i, right panels). In contrast to the primitive-streak-restricted *Egfp* transcript in the mesodermal layer, more stable LacZ enzyme activity was detected in more laterally positioned cells. This observation is consistent with the model that the cells turn off enhancer N1 before migrating laterally (Supplementary Fig. 3b). An analogous sequence of events occurs in chicken embryos⁴.

Remarkably, in the *Tbx6* mutant embryos, enhancer N1 activation persisted in the paraxial mesodermal compartment, as indicated by strong *Egfp* and LacZ expression (Fig. 2j and Supplementary Fig. 3b). Even in *Tbx6* mutants, the trans-layer cell ingress pathway seems to be confined to the primitive streak, as the laminin-positive basal lamina separating the epiblastic and mesodermal cells was interrupted only in the primitive streak region (Supplementary Fig. 3c). These observations indicate that the persistent activity of enhancer N1 in the paraxial mesodermal compartment caused ectopic *Sox2* expression, which in turn leads to the development of ectopic neural tubes. Conversely, this indicates that in normal embryos the activity of *Tbx6* expressed in the paraxial mesoderm suppresses enhancer N1 activation, thereby preventing the development of neural tubes from the mesodermal precursors.

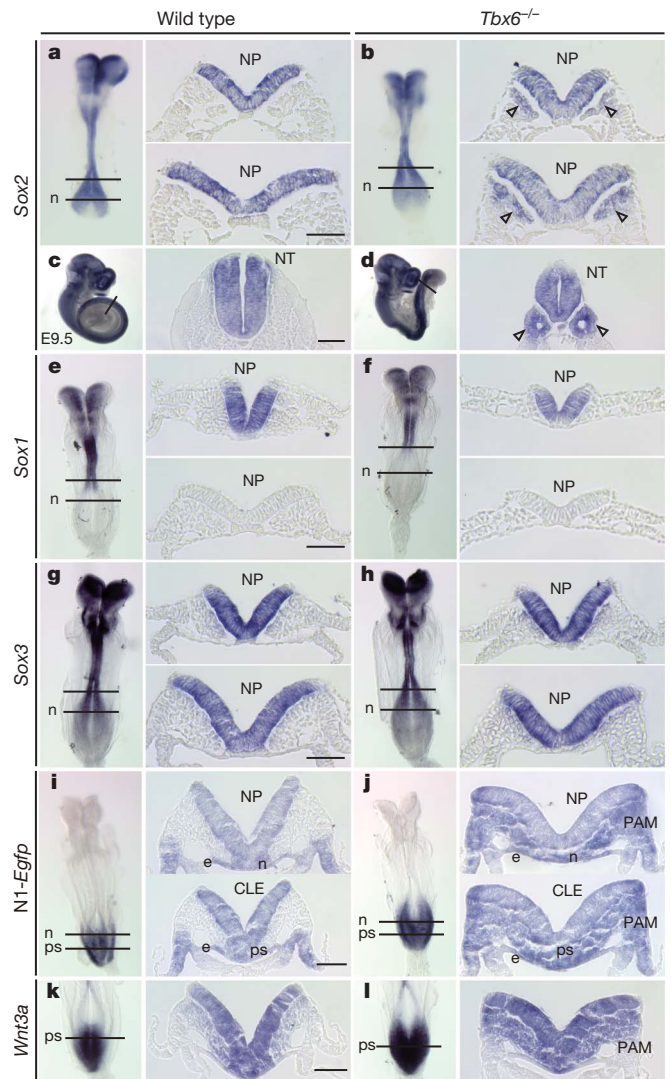


Figure 2 | Ectopic activation of enhancer N1, *Sox2* expression and neural development in the paraxial mesoderm compartment of *Tbx6*^{−/−} embryos.

a, b, *Sox2* expression in wild-type and *Tbx6*^{−/−} embryos at E8.5, shown by whole-mount *in situ* hybridization. Right panels (top and bottom) show transverse sections at the axial levels anterior to and through the node (n). NP, neural plate. Arrowheads indicate *Sox2* expression in the paraxial mesodermal compartment in *Tbx6*^{−/−} embryos. **c, d**, *Sox2* expression in wild-type and *Tbx6*^{−/−} embryos at E9.5. NT, neural tube. Arrowheads indicate development of *Sox2*-positive ectopic neural tubes. **e–h**, *Sox1* (**e, f**) and *Sox3* (**g, h**) expression in wild-type and *Tbx6*^{−/−} embryos at E8.5. **i, j**, Activity of enhancer N1 at E8.5 in wild-type embryos (**i**) or in *Tbx6*^{−/−} embryos (**j**) detected by *in situ* hybridization of *Egfp* transcripts. Right panels show transverse sections at the node (n) and primitive streak (ps) levels. In wild-type embryos, enhancer N1 activity was absent in the paraxial mesoderm compartments (PAM; **i**, right panels), whereas strong N1 activity was demonstrated in the PAM in *Tbx6*^{−/−} embryos (**j**, right panels). Enhancer activity was detected in the node and endoderm (e) in either genotype. **k, l**, Expression of *Wnt3a* at E8.5 in wild-type embryos (**k**) or *Tbx6*^{−/−} embryos (**l**) detected by *in situ* hybridization, and in transverse sections (right panel) at a primitive streak level. All scale bars, 50 μ m.

To confirm that the *Sox2* misexpression in the paraxial mesoderm compartment in *Tbx6* mutant embryos—leading to supernumerary neural tube development—is due to the ectopic activation of enhancer N1, we produced an enhancer N1 mutant allele in the mouse, in which only the enhancer N1 sequence was deleted from the *Sox2* locus (Supplementary Fig. 4). Homozygosity for the enhancer N1 mutation (Δ N1/ Δ N1) caused the loss of *Sox2* expression in the ZCNP, which is the nascent neural plate positioned immediately rostral to the CLE^{1,2,12}.

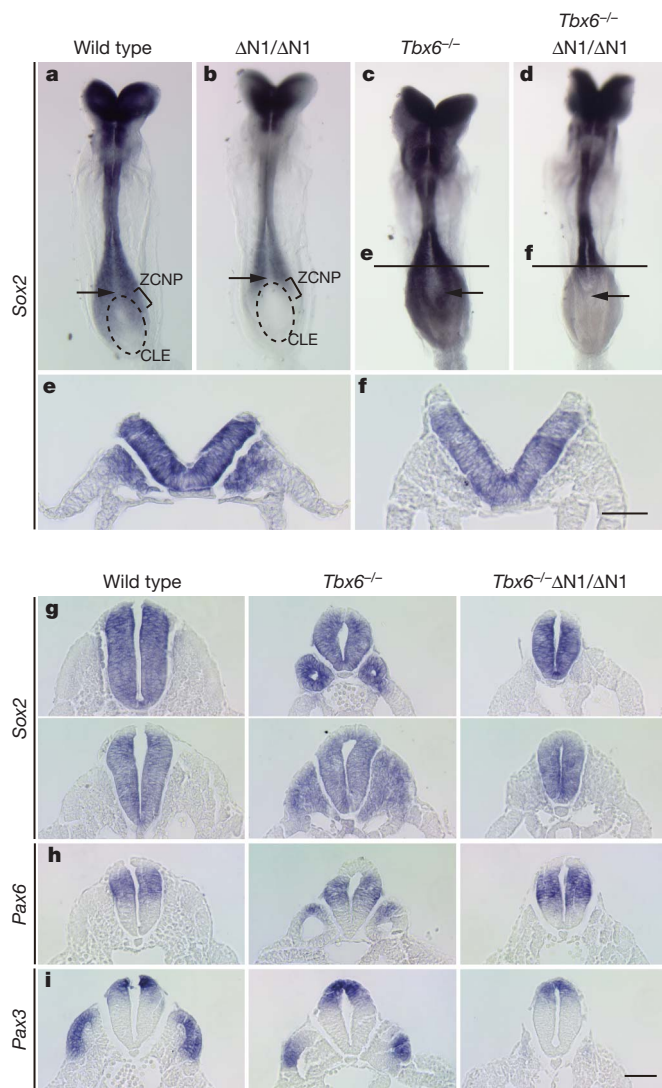


Figure 3 | Enhancer-N1-dependent paraxial *Sox2* expression and ectopic neural tube development in *Tbx6*^{-/-} embryos, and their suppression in *Tbx6*^{-/-} ΔN1/ΔN1 double mutants. **a–d**, Effects of the enhancer N1 mutation (ΔN1/ΔN1) on *Sox2* expression in the neural plate and paraxial tissues in wild-type and *Tbx6*^{-/-} embryos at E8.5. Arrows indicate the position of node. The CLE (dashed oval) and ZCNP are indicated. *Sox2* expression in the ZCNP is lost in the enhancer N1 mutant embryos. **c–f**, The loss of *Sox2* expression in the paraxial mesoderm compartment in *Tbx6*^{-/-} embryos (**e**) by the enhancer N1 mutation (**f**), demonstrated by sections of embryos of the relevant genotypes (**c**, **d**) at the axial levels indicated. Embryo specimens in **c** and **d** are overstained to confirm the absence of *Sox2* in the paraxial mesoderm compartment. **g–i**, Expression of *Sox2* (**g**, neural), *Pax6* (**h**, neural) and *Pax3* (**i**, both neural and mesodermal) was examined in embryos of respective genotypes at E9.5. All scale bars, 50 μm.

This loss of *Sox2* expression in the ZCNP in the ΔN1/ΔN1 embryos was noticeable after the 5-somite stages (E8.5) (Fig. 3b), consistent with the timing of enhancer N1 activation (Fig. 1c), and continued to E9.5. Despite this, *Sox2* was activated in the closing neural tube, and the development of the spinal cord proceeded without significant morphological defects (Fig. 3b). We presume this to be ascribable to the presence of another enhancer to back-up *Sox2* expression in the neural tube, and/or other group B1 *Sox* genes expressed in the neural plate to compensate for the role of *Sox2*.

By crossing *Tbx6*^{+/-} +/ΔN1 double heterozygotes, *Tbx6*^{-/-} ΔN1/ΔN1 double homozygous mutant embryos were successfully obtained. In *Tbx6*^{-/-} ΔN1/ΔN1 embryos at E8.5, the ectopic *Sox2* expression in the paraxial mesodermal compartment was totally absent (Fig. 3d, f),

in contrast to the case of *Tbx6*^{-/-} embryos (Fig. 3c, e), providing strong evidence that enhancer N1 determines the ectopic expression of *Sox2* in *Tbx6* mutants.

In the ectopic neural tubes that develop in *Tbx6*^{-/-} embryos at E9.5, *Sox2* expression continues, while expression of other genes that are associated with neural tube development is also initiated, namely *Sox1*, *Pax6* and *Pax3*, the latter two reflecting the dorso-ventral identity of the neural tube³ (Fig. 3 and Supplementary Fig. 5). In the *Tbx6*^{-/-} ΔN1/ΔN1 embryos at E9.5, however, the expression of all these neural genes in the paraxial compartment was extinct, concomitant with the absence of the tubular structure (Fig. 3). The paraxial tissue in the *Tbx6*^{-/-} ΔN1/ΔN1 embryos failed to express any of the mesoderm or endoderm marker genes examined, namely *Pax3* (Fig. 3i) and *Mox1* (also called *Meox1*) for paraxial mesoderm, *Pax2* for intermediate mesoderm, *Foxf1* (also called *Foxf1a*) for visceral lateral plate mesoderm, and *Foxa1* for endoderm (Supplementary Fig. 5). These observations indicate that *Tbx6* has two distinct functions in the mesodermal precursors: the inhibition of neural development by preventing enhancer N1 activation, and the promotion of mesodermal development.

To confirm that the *Sox2* misexpression in the paraxial mesoderm is causative of the ectopic neural tube development, haemagglutinin (HA)-tagged *Sox2* was ectopically expressed in the primitive paraxial mesoderm of wild-type embryos using the msd enhancer of the *Dll1* gene¹⁸ (Fig. 4a). Exogenous *Sox2*–HA was successfully expressed in the caudal-most mesodermal compartment (Fig. 4b), as indicated by HA tag immunostaining and mesodermal *Sox2* immunostaining (Fig. 4c–e). At a more rostral level of the paraxial mesoderm, where the msd enhancer activity was lost and exogenous *Sox2*–HA expression had ceased, endogenous *Sox2* expression persisted, indicating a positive feedback loop, where the former activated the latter. Notably, the clusters of cells with relatively high *Sox2* also expressed *Pax6* (Fig. 4d, open arrowheads), coincident with *Pax6* expression in the closing neural tube at the same axial level. At more rostral levels, the cells in the mesodermal compartment with an intensity of *Sox2* expression comparable to that in the neural tube formed *Pax6*-positive miniature neural tubes (Fig. 4e, white arrowheads). This result demonstrates that *Sox2* expression is sufficient for the initiation of neural tube development from the primitive paraxial mesoderm, even in wild-type embryos.

Finally, we asked whether the suppression of *Sox2* enhancer N1 activation by *Tbx6* involves direct interaction of the *Tbx6* protein with the enhancer N1 DNA sequence. Various overlapping fragments of the N1 sequence were tested for *Tbx6* binding using electrophoretic mobility shift assays (EMSA). None of the N1 subfragments exhibited T-box-factor-binding capacity, under conditions where all known T-box-binding sequences strongly bound *Tbx6* (Supplementary Fig. 6), indicating that the suppression of the enhancer N1 activity by *Tbx6* is probably not a direct regulation.

As enhancer N1 is activated by synergistic action of Wnt and Fgf signals⁴ (Fig. 1), we investigated the expression patterns of the genes encoding these protein ligands in the CLE and paraxial mesoderm^{19–22}. A remarkable change was observed in the expression pattern of *Wnt3a* (Fig. 2k, l). In normal embryos, *Wnt3a* expression is strongly expressed in the primitive streak, CLE and caudal neural plate, whereas its level is very low in the paraxial mesoderm (Fig. 2k). In *Tbx6* mutant embryos, however, the strong *Wnt3a* expression extends to the paraxial mesoderm compartment (Fig. 2l). On the other hand, the expression patterns of *Wnt8a* (absent in the mesoderm), *Fgf8* and *Fgf4* in the CLE and paraxial mesoderm compartment were not significantly altered in the *Tbx6* mutant embryos (Supplementary Fig. 7). We hypothesize that *Wnt3a* expression, normally repressed in the paraxial mesoderm, is de-repressed in the *Tbx6* mutant embryos, and the strong *Wnt3a* expression in the paraxial mesoderm is causative of the ectopic activation of enhancer N1, as shown in Fig. 4f. The strong spatial correlation between *Wnt3a* expression and enhancer N1 activity observed at various axial levels in both wild-type and *Tbx6* mutant embryos lends support for this model (Fig. 2i–l).

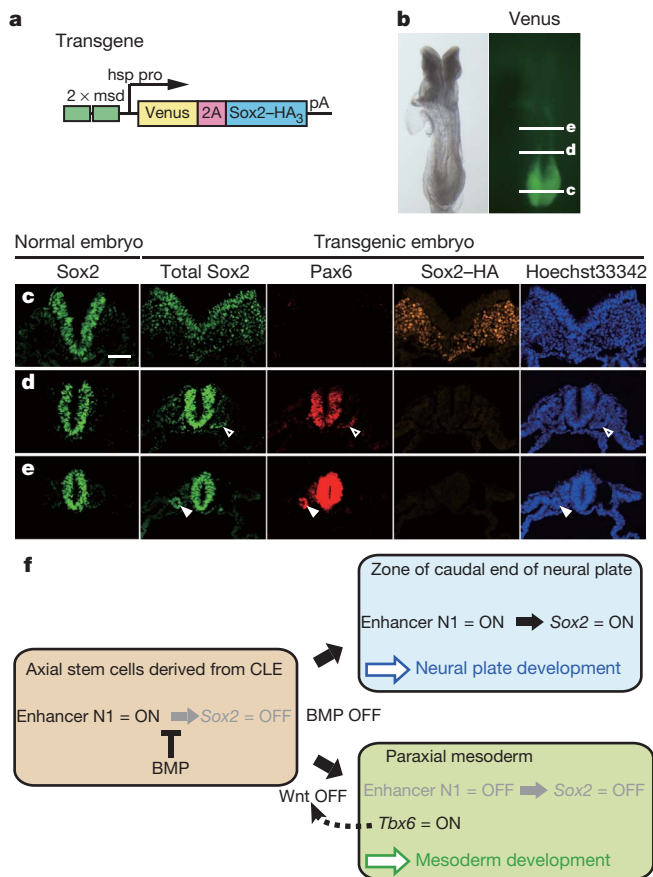


Figure 4 | Development of ectopic neural tubes from the wild-type paraxial mesoderm by misexpression of exogenous Sox2. **a**, Structure of the transgene. The msd enhancer of the gene *Dll1* (ref. 18) in a dimeric form was used for paraxial mesoderm-specific activation of the transgene coding for Venus and HA₃-tagged Sox2 joined with a 2A peptide sequence²³. **b**, Mesodermal precursor-specific activation of Venus in transgenic embryos at E8.5. **c–e**, Cross-sections at axial levels shown in **b**. Immunofluorescence for Sox2, Pax6 and HA tag, and Hoechst 33342 staining, and a comparison with Sox2 immunofluorescence of normal embryos. Scale bar, 50 μm. **f**, Model of enhancer N1 regulation and enhancer-N1-dependent Sox2 activation in normal and *Tbx6*^{-/-} embryos. In the CLE (left), where Wnt signal is above threshold, enhancer N1 is activated; however, despite this Sox2 expression itself is repressed by the inhibitory effect of BMP signals. In the ZCNP (right, top), where the Wnt signal stays ON, relief from the BMP-mediated inhibition effectuates enhancer-N1-dependent activation of Sox2 expression in the caudal neural plate. In the paraxial mesoderm (right, bottom), although the BMP signal is downregulated^{24,25}, Wnt signal drops below the threshold required for the activation of enhancer N1 when *Tbx6* activity is present, and Sox2 expression is not activated.

As discussed above, a significant fraction of the cells in the CLE domain have been shown to serve as the common precursors for the neural plate and paraxial mesoderm⁸. The present study clarifies the core regulatory circuit underlying the neural versus mesodermal dichotomous fate choice in the axial precursors, where Sox2 expression is regulated by *Tbx6* activity. As shown in Fig. 4f, the mechanism to activate Sox2 transcription operates first in CLE, namely enhancer N1 activation, and while this mechanism is still idle under the BMP-dependent Sox2 repression, a fraction of the cells migrate into the mesodermal compartment, where the activity of enhancer N1 is lost, probably due to the very low Wnt activity. *Tbx6*-dependent mesodermal development is then promoted. *Tbx6* seems to have two major functions: inhibition of Sox2 activation via enhancer N1, and activation of the mesoderm specification program. The former function is important for the latter, as Sox2 misexpression in wild-type embryos transforms

paraxial mesoderm into neural tissue (Fig. 4c–e). In the *Tbx6* mutant embryos, persistent enhancer N1 activity owing to a high Wnt3a level in the mesodermal compartment causes ectopic Sox2 expression, which is followed by expression of other neural specification genes, indicating that the Sox2 expression provides the ground state for further neural development.

The long-held view that segregation of three germ layers determines cell lineages is challenged by cell lineage analyses^{1,2,7,8} and this study, which indicate that a pool of bipotential precursor cells in the CLE serves as axial stem cells that concordantly produce neural tube and paraxial mesoderm. This characteristic of CLE is continuous with the chordo-neural hinge at later stages^{8,10}. Thus, the three germ layers describe spatial organization of tissues, but do not indicate the process of tissue derivation. Our evidence reinforces the axial stem cell model by providing the mechanistic basis for the fate choice, namely that *Tbx6*-dependent regulation of Sox2 determines the neural versus mesodermal fates in the axial stem cells derived from the CLE.

METHODS SUMMARY

In situ hybridization and immunostaining were performed to analyse the expression of relevant gene transcripts and protein products, respectively. Targeted knockout mice were used to analyse the consequence of loss in embryos of *Tbx6* and/or Sox2 enhancer N1, and transgenic mice were used to monitor enhancer N1 activity or to ectopically express Sox2. EMSA analysis was used to examine a possible interaction of *Tbx6* with enhancer N1 sequence.

Full Methods and any associated references are available in the online version of the paper at www.nature.com/nature.

Received 18 March; accepted 27 November 2010.

- Diez del Corral, R. & Storey, K. Opposing FGF and retinoid pathways: a signalling switch that controls differentiation and patterning onset in the extending vertebrate body axis. *Bioessays* **26**, 857–869 (2004).
- Wilson, V., Olivera-Martinez, I. & Storey, K. Stem cells, signals and vertebrate body axis extension. *Development* **136**, 1591–1604 (2009).
- Chapman, D. & Papaioannou, V. Three neural tubes in mouse embryos with mutations in the T-box gene *Tbx6*. *Nature* **391**, 695–697 (1998).
- Takemoto, T., Uchikawa, M., Kamachi, Y. & Kondoh, H. Convergence of Wnt and FGF signals in the genesis of posterior neural plate through activation of the Sox2 enhancer N-1. *Development* **133**, 297–306 (2006).
- Uchikawa, M., Ishida, Y., Takemoto, T., Kamachi, Y. & Kondoh, H. Functional analysis of chicken Sox2 enhancers highlights an array of diverse regulatory elements that are conserved in mammals. *Dev. Cell* **4**, 509–519 (2003).
- Kamachi, Y. *et al.* Evolution of non-coding regulatory sequences involved in the developmental process: reflection of differential employment of paralogous genes as highlighted by Sox2 and group B1 Sox genes. *Proc. Jpn. Acad. Ser. B* **85**, 55–68 (2009).
- Selleck, M. & Stern, C. Fate mapping and cell lineage analysis of Hensen's node in the chick embryo. *Development* **112**, 615–626 (1991).
- Tzouanacou, E., Wegener, A., Wymeersch, F., Wilson, V. & Nicolas, J. Redefining the progression of lineage segregations during mammalian embryogenesis by clonal analysis. *Dev. Cell* **17**, 365–376 (2009).
- Brown, J. & Storey, K. A region of the vertebrate neural plate in which neighbouring cells can adopt neural or epidermal fates. *Curr. Biol.* **10**, 869–872 (2000).
- Cambray, N. & Wilson, V. Two distinct sources for a population of maturing axial progenitors. *Development* **134**, 2829–2840 (2007).
- Mathis, L., Kulesa, P. & Fraser, S. FGF receptor signalling is required to maintain neural progenitors during Hensen's node progression. *Nature Cell Biol.* **3**, 559–566 (2001).
- Delfino-Machin, M., Lunn, J., Breitkreuz, D., Akai, J. & Storey, K. Specification and maintenance of the spinal cord stem zone. *Development* **132**, 4273–4283 (2005).
- Chapman, D., Agulnik, I., Hancok, S., Silver, L. & Papaioannou, V. *Tbx6*, a mouse T-Box gene implicated in paraxial mesoderm formation at gastrulation. *Dev. Biol.* **180**, 534–542 (1996).
- Yasuhiko, Y. *et al.* Functional importance of evolutionally conserved *Tbx6* binding sites in the presomitic mesoderm-specific enhancer of *Mesp2*. *Development* **135**, 3511–3519 (2008).
- Yasuhiko, Y. *et al.* *Tbx6*-mediated Notch signaling controls somite-specific *Mesp2* expression. *Proc. Natl Acad. Sci. USA* **103**, 3651–3656 (2006).
- Hofmann, M. *et al.* WNT signaling, in synergy with T/TBX6, controls Notch signaling by regulating *Dll1* expression in the presomitic mesoderm of mouse embryos. *Genes Dev.* **18**, 2712–2717 (2004).
- White, P. & Chapman, D. *Dll1* is a downstream target of *Tbx6* in the paraxial mesoderm. *Genesis* **42**, 193–202 (2005).
- Beckers, J. *et al.* Distinct regulatory elements direct *delta1* expression in the nervous system and paraxial mesoderm of transgenic mice. *Mech. Dev.* **95**, 23–34 (2000).

19. Bouillet, P. *et al.* A new mouse member of the *Wnt* gene family, *mWnt-8*, is expressed during early embryogenesis and is ectopically induced by retinoic acid. *Mech. Dev.* **58**, 141–152 (1996).
20. Yamaguchi, T. Genetics of Wnt signaling during early mammalian development. *Methods Mol. Biol.* **468**, 287–305 (2008).
21. Sun, X., Meyers, E., Lewandoski, M. & Martin, G. Targeted disruption of *Fgf8* causes failure of cell migration in the gastrulating mouse embryo. *Genes Dev.* **13**, 1834–1846 (1999).
22. Takada, S. *et al.* Wnt-3a regulates somite and tailbud formation in the mouse embryo. *Genes Dev.* **8**, 174–189 (1994).
23. Trichas, G., Begbie, J. & Srinivas, S. Use of the viral 2A peptide for bicistronic expression in transgenic mice. *BMC Biol.* **6**, 40 (2008).
24. Tonegawa, A. & Takahashi, Y. Somatogenesis controlled by Noggin. *Dev. Biol.* **202**, 172–182 (1998).
25. Dosch, R., Gawantka, V., Delius, H., Blumenstock, C. & Niehrs, C. Bmp-4 acts as a morphogen in dorsoventral mesoderm patterning in *Xenopus*. *Development* **124**, 2325–2334 (1997).

Supplementary Information is linked to the online version of the paper at www.nature.com/nature.

Acknowledgements We thank the members of Kondoh laboratory for discussions. This study was supported by Grants-in-Aid for Scientific Research from MEXT Japan to T.T. and H.K., an NIH grant to V.E.P., and MRC funding to R.L.-B.

Author Contributions T.T. and H.K. conceived the project; T.T. carried out major experiments; T.T. and H.K. analysed data; M.U. and M.Y. aided production and analysis of enhancer N1 mutant mice; V.E.P. provided *Tbx6* mutant mice; D.M.B., R.L.-B. and V.E.P. first indicated *Sox2* dysregulation in the *Tbx6* mutant mice; and T.T. and H.K. wrote the manuscript.

Author Information Reprints and permissions information is available at www.nature.com/reprints. The authors declare no competing financial interests. Readers are welcome to comment on the online version of this article at www.nature.com/nature. Correspondence and requests for materials should be addressed to H.K. (kondohh@fbs.osaka-u.ac.jp).

METHODS

In situ hybridization. Whole-mount *in situ* hybridization was done as previously described²⁶ with the following modifications: proteinase K treatment was done at 5 µg ml⁻¹ (E8 embryos) or 10 µg ml⁻¹ (E9 embryos) for 5 min; incubation with glycine after proteinase K treatment was omitted; digoxigenin-labelled probes were used at 0.5 µg ml⁻¹; and anti-digoxigenin antibody was reacted in 1.5% Blocking Reagent (Roche). The stained embryos were photographed in 80% Glycerol/PBT, then embedded in paraffin and sectioned. The probes used were: *Tbx6* (ref. 13), *Pax6* (ref. 27), *Uncx4.1* (ref. 28), *Foxf1* (ref. 29), *Pax2* (ref. 30), *Foxa1* (ref. 31), *Wnt8a* (ref. 32), *Fgf8* (ref. 33), *Fgf4* (ref. 34), *Sox1* 3' UTR (StuI-XhoI fragment), *Sox2* (SacII-AccI coding sequence fragment), *Sox3* (627–1,128 bp, GenBank NM_009237), *Pax3* (HindIII-PstI coding sequence fragment), *Mox1* (1,688–2,235 bp, GenBank NM_010791), *Egfp* (full coding sequence) and *Wnt3a* (a combination of probes for *Wnt3a* 3' UTR³⁵ and the *Wnt3a* coding sequence).

Immunostaining. Embryos were fixed overnight with 4% PFA in PBS, immersed in 15% and 25% sucrose in PBS in sequence for 2–3 h each step, and embedded in OCT compound. Cryosections with thickness of 10 µm were prepared, and treated at 105 °C for 15 min in antigen unmasking solution (Vector Laboratories) using an autoclave, which also quenched Venus fluorescence. The sections were reacted with 10% normal donkey serum for 30 min, then with the primary antibodies overnight at 4 °C. The primary antibodies, used at 1:200 dilutions, were: rabbit anti-laminin (L9393 Sigma), goat anti-Sox2 (AF2018 R&D Systems), rabbit anti-Pax6 (PRB-278 Covance), and rat anti-HA (1867423 Roche). After several washes, the samples were incubated with fluorescent-dye-coupled secondary antibodies for 1 h at ambient temperature. The following donkey antibodies were used at 1:200 dilutions: Alexa Fluor 488-labelled anti-goat IgG (A-11055 Molecular Probes), Alexa Fluor 555-labelled anti-rabbit IgG (A-31572 Molecular Probes), and CF 633-labelled anti-rat IgG (20137 Biotium). After several washes the samples were stained with 0.5 µg ml⁻¹ Hoechst 33342, and mounted in Permafluor (Thermo Scientific).

Transgenic mouse production, LacZ staining and embryo transfection. Transgene DNA constructs were linearized by digestion with restriction enzyme, freed from vector sequences. Injection of DNA (4 ng µl⁻¹) into the male pronucleus of fertilized eggs and LacZ enzyme staining were done using the standard procedures³⁶. Mice had genetic backgrounds derived from C57BL/6 × DBA crosses. N1-*tklacZ*⁶ and N1-*tkEgfp* were used to establish transgenic lines, whereas other transgenes were used in primary transgenic embryos. The integration of transgenes into embryo genomes was determined by PCR amplification of the *lacZ* or *Egfp/Venus* sequences from yolk sac DNA. Embryo culture and mesodermal transfection with pCAGGS-cNoggin⁴ were done as described previously³⁷.

Production of enhancer N1 mutant mice. The targeting vector used to create the enhancer N1 mutation was constructed by using a 15-kb mouse DNA fragment, which including enhancer N1, derived from the BAC clone RP23-274P9 (BACPAC Resource Center, Children's Hospital Oakland Research Institute). The STneoB cassette³⁸ was inserted 3' of enhancer N1, *loxP* sequences were inserted to flank these sequences, and a DT-A cassette³⁹ was inserted at the 3' terminus of the vector. The linearized vector was electroporated into R1 ES cells,

which had been engineered to have IRES-EGFP immediately downstream of the Sox2 ORF. Recombinants were characterized by Southern hybridization. After germline transmission from chimaeras, heterozygous mice were crossed with CAGGS-Cre mice⁴⁰ to obtain the N1-deleted allele of Sox2. A schematic of the procedure is shown in Supplementary Fig. 4.

Electrophoretic mobility shift assay. Full-length Tbx6 (436 amino acids) was synthesized using a TNT system (Promega), and EMSA analysis was performed as described previously⁴¹ using 0.1 µg µl⁻¹ poly(dI-dC) as a nonspecific competitor. The probe sequences used^{15,42,43} are indicated in Supplementary Fig. 6.

26. Wilkinson, D. G. *In situ hybridization: a practical approach* (IRL at Oxford Univ. Press, 1992).
27. Xu, P. *et al.* Regulation of Pax6 expression is conserved between mice and flies. *Development* **126**, 383–395 (1999).
28. Mansouri, A. *et al.* Paired-related murine homeobox gene expressed in the developing sclerotome, kidney, and nervous system. *Dev. Dyn.* **210**, 53–65 (1997).
29. Sawada, A. *et al.* Redundant roles of *Tead1* and *Tead2* in notochord development and the regulation of cell proliferation and survival. *Mol. Cell. Biol.* **28**, 3177–3189 (2008).
30. Dressler, G., Deutsch, U., Chowdhury, K., Nornes, H. & Gruss, P. Pax2, a new murine paired-box-containing gene and its expression in the developing excretory system. *Development* **109**, 787–795 (1990).
31. Sasaki, H. & Hogan, B. Differential expression of multiple fork head related genes during gastrulation and axial pattern formation in the mouse embryo. *Development* **118**, 47–59 (1993).
32. Kimura-Yoshida, C. *et al.* Canonical Wnt signaling and its antagonist regulate anterior-posterior axis polarization by guiding cell migration in mouse visceral endoderm. *Dev. Cell* **9**, 639–650 (2005).
33. Crossley, P. & Martin, G. The mouse *Fgf8* gene encodes a family of polypeptides and is expressed in regions that direct outgrowth and patterning in the developing embryo. *Development* **121**, 439–451 (1995).
34. Niswander, L. & Martin, G. Fgf-4 expression during gastrulation, myogenesis, limb and tooth development in the mouse. *Development* **114**, 755–768 (1992).
35. Roelink, H. & Nusse, R. Expression of two members of the Wnt family during mouse development—restricted temporal and spatial patterns in the developing neural tube. *Genes Dev.* **5**, 381–388 (1991).
36. Nagy, A., Gertsenstein, M., Vintersten, K. & Behringer, R. *Manipulating the Mouse Embryo: a Laboratory Manual* 3rd edn (Cold Spring Harbor Laboratory Press, 2003).
37. Yamamoto, M. *et al.* Nodal antagonists regulate formation of the anteroposterior axis of the mouse embryo. *Nature* **428**, 387–392 (2004).
38. Katoh, K., Takahashi, Y., Hayashi, S. & Kondoh, H. Improved mammalian vectors for high expression of G418 resistance. *Cell Struct. Funct.* **12**, 575–580 (1987).
39. Yagi, T. *et al.* A novel negative selection for homologous recombinants using diphtheria toxin A fragment gene. *Anal. Biochem.* **214**, 77–86 (1993).
40. Sakai, K. & Miyazaki, J. A transgenic mouse line that retains Cre recombinase activity in mature oocytes irrespective of the cre transgene transmission. *Biochem. Biophys. Res. Commun.* **237**, 318–324 (1997).
41. Kamachi, Y. & Kondoh, H. Overlapping positive and negative regulatory elements determine lens-specific activity of the delta 1-crystallin enhancer. *Mol. Cell. Biol.* **13**, 5206–5215 (1993).
42. Kispert, A. & Hermann, B. The Brachyury gene encodes a novel DNA binding protein. *EMBO J.* **12**, 4898–4899 (1993).
43. Conlon, F., Fairclough, L., Price, B., Casey, E. & Smith, J. Determinants of T box protein specificity. *Development* **128**, 3749–3758 (2001).